




Research Article

Chromium Ion Accumulations from Aqueous Solution by the *Eichhornia crassipes* Plant and Reusing in the Synthesis of Cr-Doped ZnO Photocatalyst

Osman Ahmed Zelekew ¹, Paulos Asefa Fufa,¹ Fedlu Kedir Sabir ²,
Dinsefa Mensur Andoshe,¹ Noto Susanto Gultom ³, Hairus Abdellah,³ Dong-Hau Kuo,³
Xiaoyun Chen,⁴ and Gopal Krishna Devulapalli²

¹Department of Materials Science and Engineering, Adama Science and Technology University, Adama, Ethiopia

²Department of Applied Chemistry, Adama Science and Technology University, Adama, Ethiopia

³Department of Materials Science and Engineering, National Taiwan University of Science and Technology, Taipei 10607, Taiwan

⁴College of Materials Engineering, Fujian Agriculture and Forestry University, Fuzhou 350002, China

Correspondence should be addressed to Osman Ahmed Zelekew; osmax2007@gmail.com

Received 23 October 2021; Revised 9 February 2022; Accepted 24 February 2022; Published 8 March 2022

Academic Editor: Van Viet Pham

Copyright © 2022 Osman Ahmed Zelekew et al. This is an open access article distributed under the Creative Commons Attribution License, which permits unrestricted use, distribution, and reproduction in any medium, provided the original work is properly cited.

The Cr-doped ZnO photocatalysts were synthesized through the chromium ion accumulations by water hyacinth (*Eichhornia crassipes*). In the preparation process, the plant tissues were immersed in different sample flasks containing chromium precursors for 1, 2, 4, 6, and 8 days. The plant tissue containing chromium ion was mixed with zinc precursor followed by calcinations. For simplicity, the prepared Cr-doped ZnO samples with the plant immersed for 1, 2, 4, 6, and 8 days were abbreviated as D1, D2, D4, D6, and D8, respectively. Moreover, pure ZnO was also prepared without the water hyacinth plant accumulated with chromium ion for comparison purposes. The powder sample characterizations were performed and evaluated in the degradation of methylene blue (MB). The Cr-doped ZnO sample (D1) degrades 80% of MB dye while the D2, D4, D6, D8, and pure ZnO samples degrade only 74, 76, 79, 73, and 25%, respectively. On the other hand, without the addition of catalysts (blank), there was no significant degradation of MB dye within 90 min irradiation. Therefore, the degradation performance of Cr-doped ZnO in the presence of optimum amount of chromium dopant and water hyacinth is highly improved than that of pure ZnO. The catalytic improvement may be as a result of reducing the photogenerated electron and hole recombination rates due to the presence of dopants. Moreover, the presence of the *Eichhornia crassipes* plant in the synthesis of Cr-doped ZnO could also prevent further aggregations and particle size growth and enhance the porosity after calcination.

1. Introduction

Currently, the disposals of industrial effluents without proper treatment are the major threat and the utmost research areas in the world [1, 2]. Mainly, organic and inorganic wastes released from different sectors such as textile industries, dyeing, paintings, and other sources are the potential causes of water pollutions [3, 4]. Hence, proper controls of pollutants

discharged from different sources with appropriate removal techniques should be the primary activity [5–8]. One of the techniques used in the wastewater treatment technology is photocatalysis. In the photocatalysis process, semiconductors such as ZnO can be used due to the ability to absorb the light, nontoxicity, and stability [9–11]. However, the activity of the ZnO semiconductor on the visible light source is not good due to its larger band gap energy (3.2 eV) [12, 13]. Due to this

reason, different modifications have been employed to enhance the photocatalytic activity performances of the ZnO semiconductor [14, 15].

Currently, reports on a ZnO-based photocatalyst are available [15–18]. For example, the prepared ZnO from *Acremonium potronii* for dye degradation was reported by Ameen et al. [19]. The hexavalent chromium and dye degradations were also performed by using ZnO under UV light [20]. However, ZnO alone is not effective under visible light irradiation. Due to this reason, a lot has been done on the photocatalytic performance improvements of ZnO [21, 22]. Among the reported performance improvements of ZnO are doping with metal [23, 24], nonmetals [25], and ZnO combination with other low band gap energy semiconductors [26]. Specifically, Cr-doped ZnO photocatalysts were also synthesized and used for organic dye degradation [27, 28]. However, further catalytic performance improvements of ZnO by using a green synthesis method are also needed. For this purpose, the biological renewable plant materials can be used as a template to prepare oxide semiconductor-based photocatalysts [29, 30]. Among the biological renewable unwanted plant materials resources is *Eichhornia crassipes*.

Recently, *Eichhornia crassipes* is used for pollutant removal [31, 32]. For example, pollutant removal via phytoremediation techniques using water hyacinth from wastewater was studied by Rezaia et al. [33]. The removal of Pb^{2+} , Zn^{2+} , and Ni^{2+} , with water hyacinth fiber, was also reported [34]. Additionally, the cadmium ion, Cu^{2+} , and chromium (VI) ion heavy metal removal with water hyacinth-based biochar, chitosan materials, and water hyacinth roots, respectively, were also tested and showed good removal efficiencies [35–37]. Moreover, recycling performance of the heavy metals after accumulation on water hyacinth was also studied [38]. In our previous report, the cobalt ion accumulations onto *Eichhornia crassipes* for the purpose of cobalt doping on ZnO were also studied [39]. However, there was no report on the chromium ion accumulations onto water hyacinth and recycled for organic pollutant degradations.

Herein, the water hyacinth was immersed into chromium aqueous solution to collect the chromium ion on the surface of the plant tissue. The chromium ion-containing plant was mixed with a zinc precursor to prepare Cr-doped ZnO after calcinations in air. The remained amount of chromium ion in the aqueous solution was measured. The Cr-doped ZnO powder catalyst characterizations were performed. The catalytic performance of Cr-doped ZnO was tested. Here, the chromium ion removal efficiency of water hyacinth from aqueous solution was evaluated. Moreover, the reusing of the accumulated chromium ion on the plant as a dopant for ZnO preparation in the decontamination of organic pollutants was also studied systematically. Pure ZnO only was prepared and tested in the degradation of MB dye for comparison purpose. It is suggested that the Cr-doped ZnO performance could have better catalytic activity than pure ZnO due to widening the visible light absorption, electron/hole separation, and improving the porosity of the materials as a result of *Eichhornia crassipes* after calcination.

TABLE 1: The chromium ion concentration remained after being accumulated for different days.

Soaking days	Remained chromium ion concentration (mg/L)	Amount of chromium ion accumulated (mg/L)
Initial solution	1725.00	—
D1	1625.00	100.00
D2	1632.50	92.50
D4	1503.50	221.50
D6	1511.25	213.75
D8	1498.75	226.25

2. Materials and Methods

2.1. Chemicals and Reagent. Potassium dichromate ($K_2Cr_2O_7$) (Sigma-Aldrich), zinc nitrate hexahydrate ($Zn(NO_3)_2 \cdot 6H_2O$) (Sigma-Aldrich), sodium hydroxide (NaOH) (Loba Chemie), and ethanol were used in the experimental work. The chemicals used for the experiment were of analytical grade.

2.2. Preparation of the Water Hyacinth. The *Eichhornia crassipes* plant was brought from Lake Koka, Ethiopia. The plant was washed with water to remove dusts from the surface. It was dried at room temperature, crushed, and stored for further use.

2.3. Preparation of Cr-Doped ZnO. The crushed powder plant (2 g) was added into a chromium solution at different days (1, 2, 4, 6, and 8) in separate flasks. Then, the *Eichhornia crassipes* having chromium ion on the surface was separated. The supernatant solution was tested with a microwave plasma atomic emission spectrometer (MP-AES) (Agilent, Germany) to examine the remaining chromium ion content in the solution. For comparison purpose, the initial concentration of chromium ion (before soaking of the plant) was also measured by MP-AES. The plant having chromium ion was dried and mixed with 80 mL of zinc nitrate (0.5 M) precursor. Then, the sample was stirred and heated at 80°C for 2 h, followed by adjusting the pH to 10. Then, the solution was centrifuged, washed, and dried followed by calcination in air at 600°C for 3 h.

2.4. Characterizations. X-ray diffraction (XRD) was illustrated by Shimadzu XRD-7000. The field emission scanning electron microscopy (FESEM, JSM 6500F, JEOL) was used for morphology analysis. ESCALAB 250 for X-ray photoelectron spectroscopy (XPS) analysis was used to determine the oxidation states in the powder. The diffuse reflectance spectroscopy (DRS) was evaluated using a JASCO V-670UV-Vis spectrophotometer. The photoluminescence behaviors of the materials were characterized with a JASCD FB-8500 fluorescence spectrophotometer. Fourier transform infrared (FTIR) analysis was performed with Spectrum 65 FT-IR (PerkinElmer) using KBr pellets. The concentration of the pollutants before and after photocatalytic reactions was measured by using a Shimadzu-3600 Plus spectrophotometer.

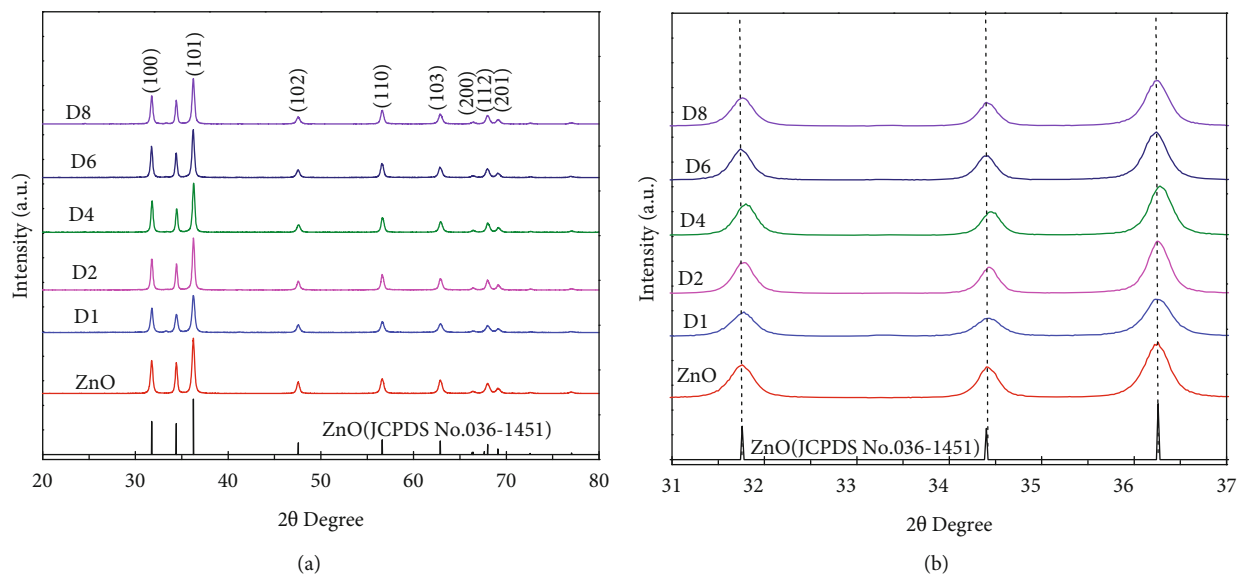


FIGURE 1: XRD patterns of (a) ZnO (JCPDS No. 036-1451), ZnO, D1, D2, D4, D6, and D8 samples and (b) 2θ from $31-37^\circ$ range.

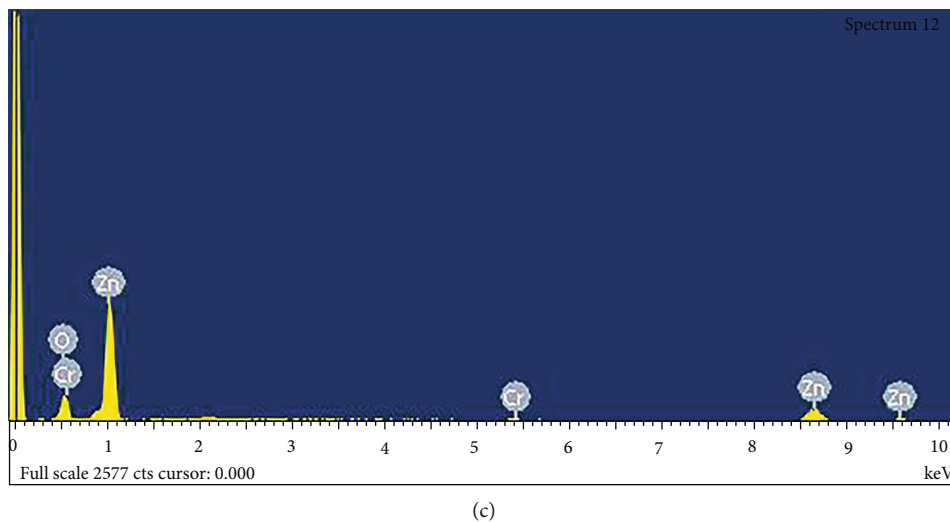
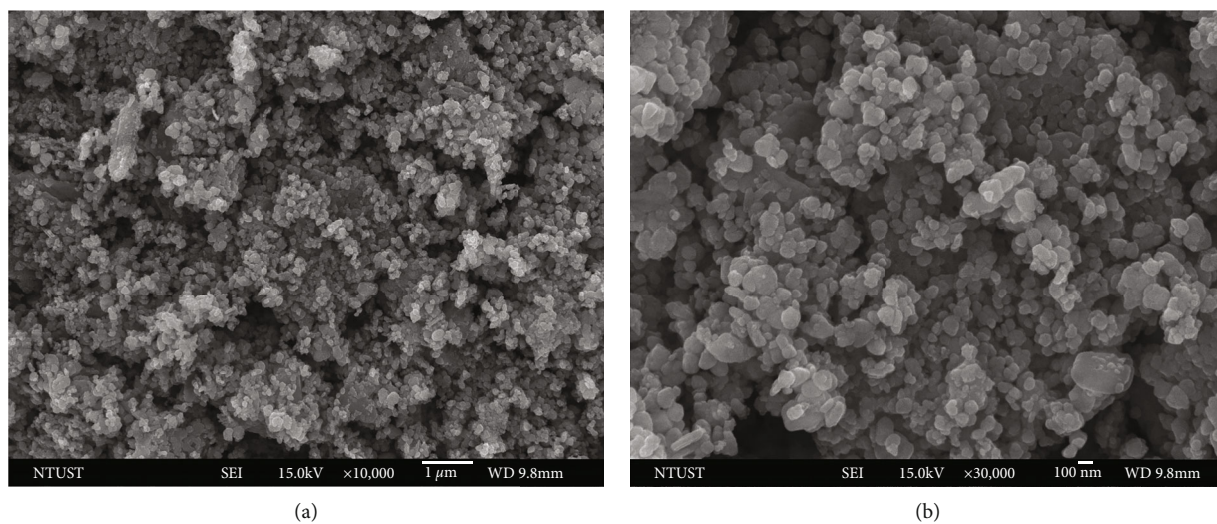


FIGURE 2: (a, b) SEM image of lower and higher resolution and (c) EDS analysis for the D1 sample.

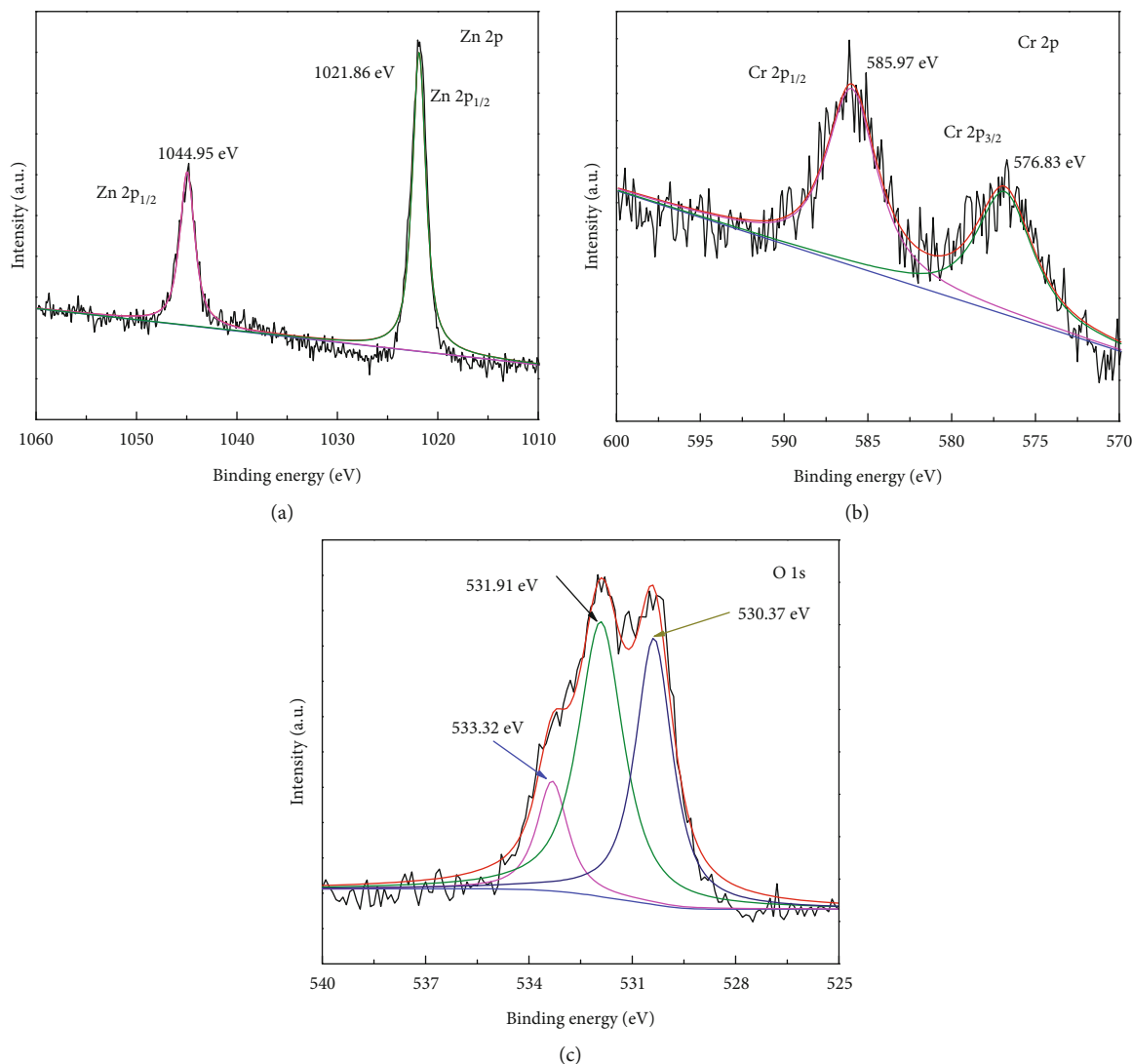


FIGURE 3: The XPS analysis of (a) Zn 2p, (b) Cr 2p, and (c) O 1s for the D1 sample.

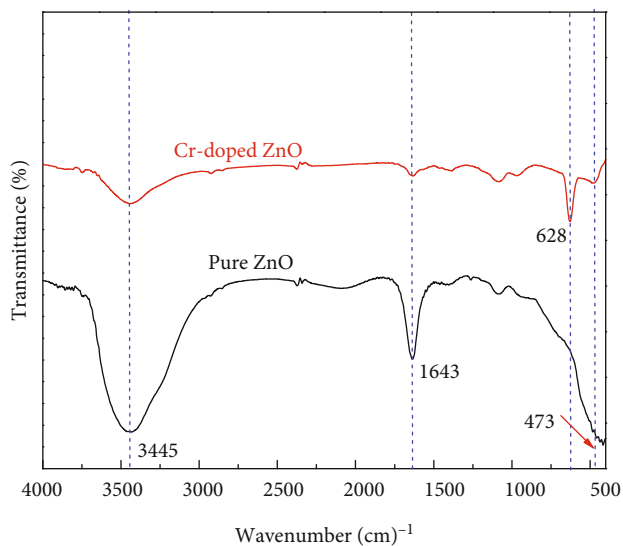


FIGURE 4: FTIR analysis of pure ZnO and Cr-doped ZnO catalysts.

2.5. Photocatalytic Activities. MB dye was used as a pollutant to test the photocatalytic performance of the prepared samples according to the reported literature with modification [18]. In the degradation test, Cr-doped ZnO (25 mg) was mixed into 10 ppm of 100 mL dye solution. Adsorption/desorption experiment was performed for 30 min under stirring in the dark condition. Then, a light source (visible light) was on after 30 min adsorption/desorption reaction with continuous stirring. Finally, 5 mL of the aliquot sample was taken out at 15 min intervals of time and used for analysis after centrifugation. For comparison purposes, the degradation of the pollutant was performed in the presence of pure ZnO and blank (without catalyst) with the same procedure as mentioned above.

3. Results and Discussion

After soaking the *Eichhornia crassipes* plant in the chromium ion solution for different days, the plant materials accumulated with chromium ion was separated and the

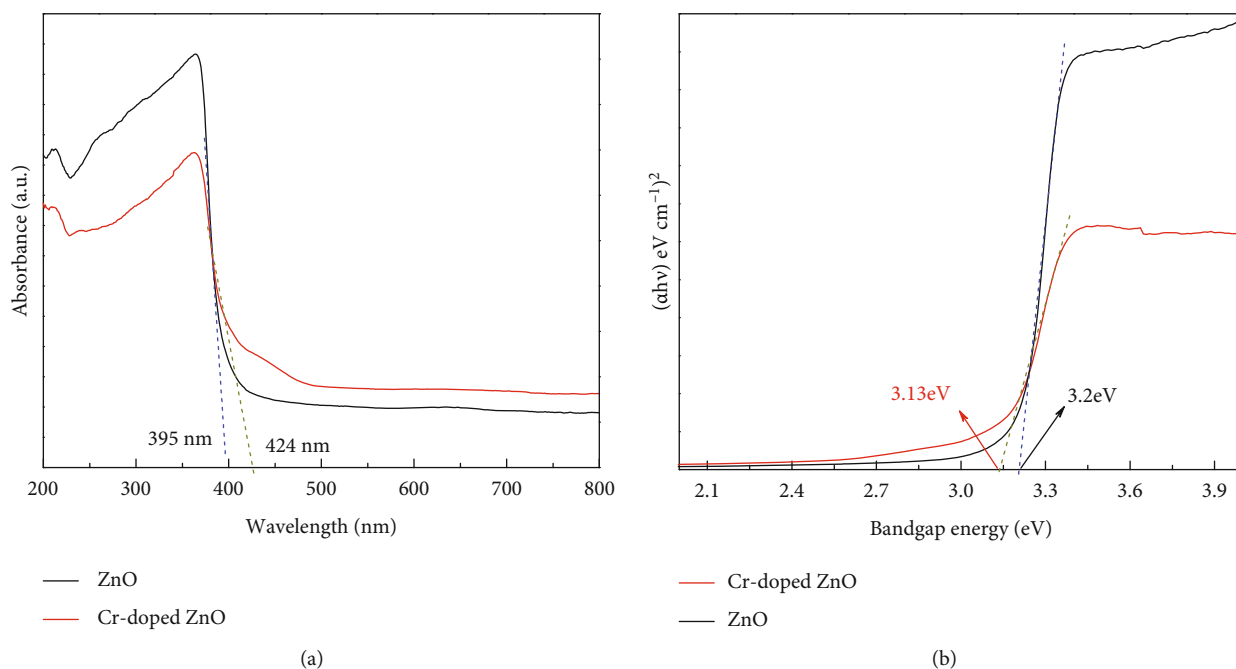


FIGURE 5: (a) UV-visible spectra and (b) band gap for pure ZnO and Cr-doped ZnO samples.

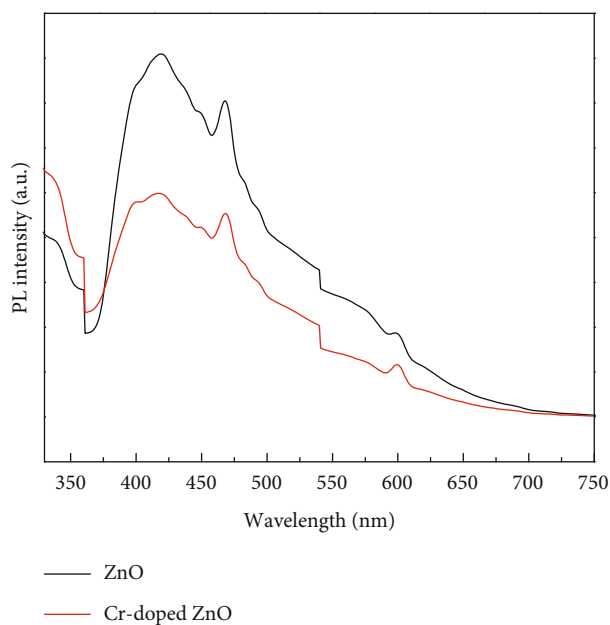


FIGURE 6: Photoluminescence (PL) spectra of pure ZnO and Cr-doped ZnO.

remaining aqueous solution in the sample flasks was subjected to MP-AES measurement. For comparison purpose, the initial chromium solution was also measured. The initial concentration of chromium ion was 1725.00 mg/L. However, after chromium ion accumulations, the concentrations in the solution were decreased which indicated that the *Eichhornia crassipes* plant tissue has the ability to accumulate the chromium ion. Table 1 shows the initial concentration and remained and accumulated amount of chromium ion on water *Eichhornia crassipes* tissue for each day.

The XRD analysis was performed for the powder samples. Figure 1 indicates the XRD patterns for reference ZnO (JCPDS No.036-1451) and D1, D2, D4, D6, and D8 samples. As it is observed from Figure 1, all the samples had ZnO hexagonal wurtzite structure with (100), (002), (101), (102), (110), (103), (200), (112), and (201) planes (JCPDS No. 036-1451). There were no other peaks observed from chromium oxides or any other related phases in which the prepared samples were ZnO. The results showed that the structure of ZnO crystal was not affected by adding Cr atoms which indicates that the Zn sites were substituted by Cr in the lattices as it is reported Cr-doped ZnO [40]. Moreover, in the presence of the water hyacinth plant accumulated with chromium ion, the XRD was shifted to the higher angle as it is illustrated from Figure 1(b) in the 31-37° range. This magnificent shifting could be due to the incorporation of Cr^{3+} into the ZnO lattice. On the other hand, it is expected that Cr^{3+} ions can replace Zn^{2+} ions due to the smaller radius (0.063 nm) of Cr^{3+} ions as compared to the radius (0.074 nm) of Zn^{2+} ions [41].

Figure 2 indicates the SEM images at lower (Figure 2(a)) and higher (Figure 2(b)) resolution and EDS (Figure 2(c)) analysis for sample D1, respectively. As it is indicated in the SEM image, smaller and well-dispersed spherical nanoparticles were observed. The SEM showed that the presence of water hyacinth in the preparation process could prevent the agglomeration and reduces the particle size which also indicates better catalytic performance. Moreover, EDS analysis also indicates Zn, Cr, and O elements in the sample which confirms the preparation of Cr-doped ZnO.

The powder sample of the Cr-doped ZnO (D1) was also further characterized by XPS. Figure 3(a) illustrates the presence of the Zn^{2+} in the sample with 1021.86 and 1044.95 eV binding energies for Zn $2p_{3/2}$ and Zn $2p_{1/2}$,

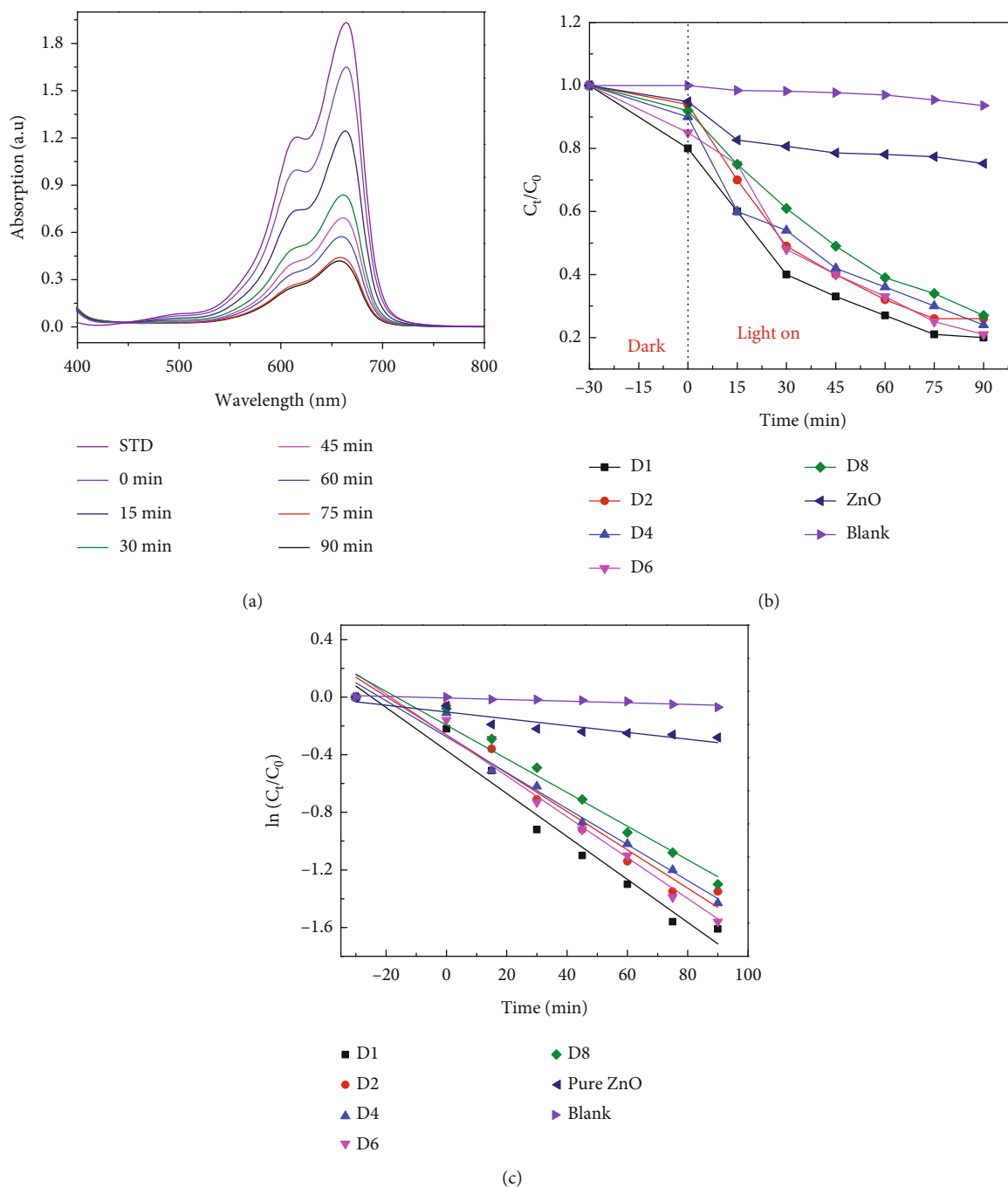


FIGURE 7: (a) UV-visible absorption spectra for D1, (b) C_t/C_0 , and (c) the first-order kinetic plots for D1, D2, D4, D6, D8, pure ZnO, and blank samples.

respectively [42]. Moreover, the 576.83 and 585.97 eV binding energies for Cr $2p_{3/2}$ and Cr $2p_{1/2}$, respectively, indicate the Cr^{3+} (Figure 3(b)) [43, 44]. On the other hand, the O 1s XPS peaks indicated at 530.37, 531.91, and 533.32 eV binding energies illustrate Zn-O and Cr-O of lattice oxygen and oxygen vacancy, respectively (Figure 3(c)) [45–47]. The result further confirms successful preparation of the Cr-doped ZnO.

The FTIR analysis was also performed for further exploring the structural properties of the samples. Figure 4

indicates the FTIR data for pure ZnO and Cr-doped ZnO samples. The FTIR spectra exhibiting a band about 628 cm^{-1} for the Cr-doped ZnO sample could be assigned to O-Cr-O [40]. The absorption peaks showed at ~ 3457 and 1643 cm^{-1} indicate the stretching and bending vibration mode of O-H as a result of water molecule adsorbed on the prepared sample surface. Moreover, the FTIR peak at $\sim 473\text{ cm}^{-1}$ indicates the stretching vibrational mode of the Zn-O bond [39, 48]. The results indicate that the Cr-doped ZnO catalyst was synthesized successfully.

TABLE 2: Comparison of photocatalytic activity of Cr-doped ZnO with related literature in the degradation of MB dye.

Catalyst	Weight (g)	Concentration (ppm)	Time (min)	Degradation (%)	Ref.
Fe ₃ O ₄ /ZnO	0.20	100	120	88.5	[53]
2%Fe-ZnO	1.00	10	180	92	[54]
ZnO NPs	0.02	10	150	94	[55]
NiO-ZnO	0.18	10	120	74.86	[56]
Cr-doped ZnO (D1)	0.025	10	90	80	This work

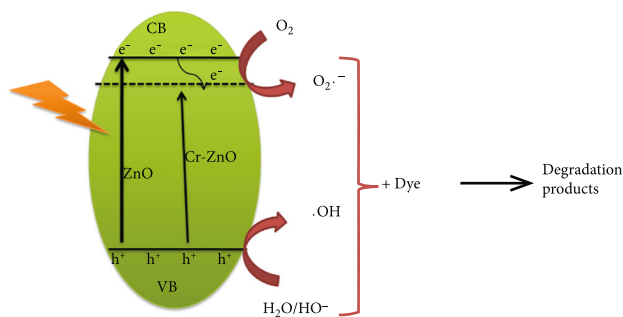


FIGURE 8: The degradation mechanisms of MB dye with the Cr-doped ZnO photocatalyst.

The absorption properties of pure ZnO and Cr-doped ZnO catalysts were studied as shown in Figure 5(a). The pure ZnO had an absorption edge at about 395 nm. After Cr doping, the absorption edge was shifted to 424 nm. Moreover, the absorption of Cr-doped ZnO becomes relatively higher than that of pure ZnO in the visible region. The band gaps for pure ZnO and Cr-doped ZnO were also calculated and shown as 3.2 and 3.13 eV, respectively (Figure 5(b)). The result indicates that the presence of Cr as a dopant in the ZnO lattice plays the major role for enhancing the catalytic activity. On the other hand, the Cr-doped ZnO performance could have better catalytic activity than pure ZnO due to widening the visible light absorption and electron and hole separation [49].

The photoluminescence (PL) analysis was also performed as shown in Figure 6. The PL measurements were obtained at 325 nm excitation wavelength. The decrease in the PL band intensity was observed in the Cr-doped ZnO. It is reported that the higher the intensity band in the PL analysis, the higher the electron and hole recombination rate of the samples [7]. It is observed that the PL intensity of Cr-doped ZnO is smaller than that of pure ZnO, indicating that Cr doping has the ability to increase the defects and oxygen vacancies in the ZnO sample [50]. It is also known that any compound having a lower PL intensity band and a long lifetime will have a good photocatalytic activity since the separation of photogenerated electron and hole pairs will be easy [51].

The catalytic activities of the prepared powders were checked in the MB dye degradation as shown in Figure 7. Figure 7(a) indicates the UV-visible absorption spectral measurements at different interval reaction times for sample D1. Moreover, Figure 7(b) shows the C_t/C_0 ratio plots for D1, D2, D4, D6, D8, pure ZnO, and blank (without catalyst)

samples. As it is indicated from Figure 7(b), the Cr-doped ZnO accumulated for one day (D1) degrades 80% of MB dye. However, the D2, D4, D6, D8, and pure ZnO samples degrade only 74, 76, 79, 73, and 25%, respectively. On the other hand, without the addition of catalysts (blank), there was no significant degradation of MB dye within 90 min irradiation. It is illustrated that the Cr ion incorporated into the ZnO lattice from chromium-accumulated *Eichhornia crassipes* with optimum amount enhances the photocatalytic performance. Figure 7(c) indicates a plot for $\ln(C_t/C_0)$ with irradiation time in the MB dye degradation. The degradation indicates the pseudo-first-order kinetics which is also similar to the literature report [52]. The rate constants of D1, D2, D4, D6, D8, and pure ZnO samples were also calculated and shown as 0.0149, 0.0133, 0.0125, 0.0142, 0.0117, and 0.0024 min^{-1} , respectively. As it is shown from the result, the maximum rate constant was obtained from the D1 sample in which the D1 was the best catalyst in the MB degradation. Moreover, the ratio constant (K) for the D1 sample was also calculated and estimated to be 0.596 $\text{min}^{-1} \text{g}^{-1}$. Moreover, the catalytic performance was also compared with literature as shown in Table 2. It is suggested the catalytic performance is comparable with literature reports.

Figure 8 indicates the mechanism for MB dye oxidation with the Cr-doped ZnO catalyst. As it is reported, the photocatalyst absorbs the irradiated light to generate electron and hole pairs. When semiconductor photocatalysts are subjected to light irradiation, there will be excitation of electrons into the conduction band (CB). The photogenerated holes will be remained in the VB [57]. When ZnO is doped with chromium, the electrons will be trapped and the recombination of the hole and electron could be suppressed as it is also reported in metal-doped ZnO [15, 58]. The electron-hole pairs on the surface of the photocatalyst pass through a series of oxidation-reduction reactions affecting the organic pollutant molecules. For example, the photogenerated electrons can interact with adsorbed O_2 , on the surface of the sample, and generate a superoxide radical anion ($\text{O}_2^{\bullet-}$). Moreover, due to the presence of oxygen vacancies as it is illustrated from the XPS results, there will be better absorption of O_2 which is a source of superoxide radical anion [51]. The photogenerated holes can also interact with hydroxyl ion (OH^-) or H_2O to generate hydroxyl radical (OH^\bullet) [15, 27, 59]. The reactive oxygen species resulting from the reaction will be interacted with MB dye and degrades into smaller degradation products [39, 59]. Figure 8 illustrates the mechanism for MB dye oxidation with the Cr-doped ZnO catalyst.

4. Conclusion

The Cr-doped ZnO was prepared via the chromium ion accumulation with the *Eichhornia crassipes* plant for one, two, four, six, and eight days and mixed with a zinc precursor. In this report, the removal of chromium ion and reusing it again for the purpose of a dopant in the ZnO photocatalyst synthesis were illustrated. The prepared materials were also tested for MB dye degradation. The chromium ion accumulated for one day and mixed with a zinc precursor followed by calcination (D1) showed the best catalytic performance and degrades 80% of MB dye while D2, D4, D6, D8, and pure ZnO samples degrade only 74, 76, 79, 73, and 25% of MB dye, respectively. Therefore, degradation of the organic pollutants with Cr-doped ZnO with the aid of a plant accumulated with chromium ion was efficient. The catalytic performance enhancement may be as a result of reducing recombination rates of the electrons and hole, the particle size reduction, and porosity improvement resulting from the water hyacinth plant after calcination.

Data Availability

The data used to support the findings of this study are included within the article.

Conflicts of Interest

The authors declare that there are no conflicts of interest regarding the publication of this paper.

Acknowledgments

This research work was supported by Adama Science and Technology University (ASTU) under grant no. ASTU/ASR/001/2019. The authors also want to acknowledge the National Taiwan University of Science and Technology Department of Materials Science and Engineering for DRS, PL, SEM/EDS, and XPS analysis.

References

- [1] O. Ahmed Zelekew and D. H. Kuo, "A two-oxide nanodiode system made of double-layered p-type Ag_2O @n-type TiO_2 for rapid reduction of 4-nitrophenol," *PCCP*, vol. 18, no. 6, pp. 4405–4414, 2016.
- [2] P. Bhatia and M. Nath, "Green synthesis of p-NiO/n-ZnO nanocomposites: excellent adsorbent for removal of congo red and efficient catalyst for reduction of 4-nitrophenol present in wastewater," *Journal of Water Process Engineering*, vol. 33, article 101017, 2020.
- [3] X. Chen, H. Sun, O. A. Zelekew et al., "Biological renewable hemicellulose-template for synthesis of visible light responsive sulfur-doped TiO_2 for photocatalytic oxidation of toxic organic and As(III) pollutants," *Applied Surface Science*, vol. 525, article 146531, 2020.
- [4] O. A. Zelekew and D.-H. Kuo, "Synthesis of a hierarchical structured NiO/NiS composite catalyst for reduction of 4-nitrophenol and organic dyes," *RSC Advances*, vol. 7, no. 8, pp. 4353–4362, 2017.
- [5] D. Lu, O. A. Zelekew, A. K. Abay, Q. Huang, X. Chen, and Y. Zheng, "Synthesis and photocatalytic activities of a CuO/ TiO_2 composite catalyst using aquatic plants with accumulated copper as a template," *RSC Advances*, vol. 9, no. 4, pp. 2018–2025, 2019.
- [6] Y. Fan, H. Zhang, M. Ren et al., "Low-temperature catalytic degradation of chlorinated aromatic hydrocarbons over bimetallic Ce-Zr/UiO-66 catalysts," *Chemical Engineering Journal*, vol. 414, article 128782, 2021.
- [7] O. A. Zelekew, D.-H. Kuo, J. M. Yassin, K. E. Ahmed, and H. Abdullah, "Synthesis of efficient silica supported $\text{TiO}_2/\text{Ag}_2\text{O}$ heterostructured catalyst with enhanced photocatalytic performance," *Applied Surface Science*, vol. 410, pp. 454–463, 2017.
- [8] H. Sun, A. B. Abdeta, O. A. Zelekew et al., "Spherical porous SiO_2 supported CuVOS catalyst with an efficient catalytic reduction of pollutants under dark condition," *Journal of Molecular Liquids*, vol. 313, article 113567, 2020.
- [9] R. Behnood and G. Sodeifian, "Synthesis of N doped-CQDs/Ni doped-ZnO nanocomposites for visible light photodegradation of organic pollutants," *Journal of Environmental Chemical Engineering*, vol. 8, no. 4, article 103821, 2020.
- [10] S. Zarezadeh, A. Habibi-Yangjeh, and M. Mousavi, "BiOBr and AgBr co-modified ZnO photocatalyst: a novel nanocomposite with p-n-n heterojunctions for highly effective photocatalytic removal of organic contaminants," *Journal of Photochemistry and Photobiology A: Chemistry*, vol. 379, pp. 11–23, 2019.
- [11] P. Raizada, J. Kumari, P. Shandilya, and P. Singh, "Kinetics of photocatalytic mineralization of oxytetracycline and ampicillin using activated carbon supported ZnO/ ZnWO_4 nanocomposite in simulated wastewater," *Desalination and Water Treatment*, vol. 79, pp. 204–213, 2017.
- [12] M. Samadi, M. Zirak, A. Naseri, E. Khorashadizade, and A. Z. Moshfegh, "Recent progress on doped ZnO nanostructures for visible-light photocatalysis," *Thin Solid Films*, vol. 605, pp. 2–19, 2016.
- [13] S. Shaker-Agjekandy and A. Habibi-Yangjeh, "Ultrasonic-assisted preparation of novel ternary ZnO/AgI/ Ag_2CrO_4 nanocomposites as visible-light-driven photocatalysts with excellent activity," *Materials Science in Semiconductor Processing*, vol. 44, pp. 48–56, 2016.
- [14] C. Wu, L. Shen, Y.-C. Zhang, and Q. Huang, "Solvothermal synthesis of Cr-doped ZnO nanowires with visible light-driven photocatalytic activity," *Materials Letters*, vol. 65, no. 12, pp. 1794–1796, 2011.
- [15] T. K. Truong, T. Van Doan, H. H. Tran et al., "Effect of Cr doping on visible-light-driven photocatalytic activity of ZnO nanoparticles," *Journal of Electronic Materials*, vol. 48, no. 11, pp. 7378–7388, 2019.
- [16] O. A. Zelekew, P. A. Fufa, F. K. Sabir, and A. D. Duma, "Water hyacinth plant extract mediated green synthesis of $\text{Cr}_2\text{O}_3/\text{ZnO}$ composite photocatalyst for the degradation of organic dye," *Heliyon*, vol. 7, no. 7, article e07652, 2021.
- [17] P. Basnet, D. Samanta, T. I. Chanu, and S. Chatterjee, "Visible light facilitated degradation of alternate dye solutions by highly reusable Mn-ZnO nano-photocatalyst," *Journal of Alloys and Compounds*, vol. 867, article 158870, 2021.
- [18] S. G. Aragaw, F. K. Sabir, D. M. Andoshe, and O. A. Zelekew, "Green synthesis of p- $\text{Co}_3\text{O}_4/\text{n-ZnO}$ composite catalyst with *Eichhornia crassipes* plant extract mediated for methylene

- blue degradation under visible light irradiation," *Materials Research Express*, vol. 7, no. 9, article 095508, 2020.
- [19] F. Ameen, T. Dawoud, and S. AlNadhari, "Ecofriendly and low-cost synthesis of ZnO nanoparticles from *Acremonium potronii* for the photocatalytic degradation of azo dyes," *Environmental Research*, vol. 202, article 111700, 2021.
- [20] M. V. Kangralkar, J. Manjanna, N. Momin, K. S. Rane, G. P. Nayaka, and V. A. Kangralkar, "Photocatalytic degradation of hexavalent chromium and different staining dyes by ZnO in aqueous medium under UV light," *Monitoring & Management*, vol. 16, article 100508, 2021.
- [21] S. K. Jena, R. Sadasivam, G. Packirisamy, and P. Saravanan, "Nanoremediation: sunlight mediated dye degradation using electrospun PAN/CuO-ZnO nanofibrous composites," *Environmental Pollution*, vol. 280, article 116964, 2021.
- [22] L. Gnanasekaran, R. Hemamalini, R. Saravanan et al., "Synthesis and characterization of metal oxides (CeO₂, CuO, NiO, Mn₃O₄, SnO₂ and ZnO) nanoparticles as photo catalysts for degradation of textile dyes," *Journal of Photochemistry and Photobiology B: Biology*, vol. 173, pp. 43–49, 2017.
- [23] R. Beura, S. Rajendran, M. A. Gracia Pinilla, and P. Thangadurai, "Enhanced photo-induced catalytic activity of Cu ion doped ZnO - graphene ternary nanocomposite for degrading organic dyes," *Journal of Water Process Engineering*, vol. 32, article 100966, 2019.
- [24] I. Ahmad, "Comparative study of metal (Al, Mg, Ni, Cu and Ag) doped ZnO/g-C₃N₄ composites: efficient photocatalysts for the degradation of organic pollutants," *Separation and Purification Technology*, vol. 251, article 117372, 2020.
- [25] H. Sudrajat and S. Babel, "A novel visible light active N-doped ZnO for photocatalytic degradation of dyes," *Journal of Water Process Engineering*, vol. 16, pp. 309–318, 2017.
- [26] A. Ghosh and A. Mondal, "Fabrication of stable, efficient and recyclable p-CuO/n-ZnO thin film heterojunction for visible light driven photocatalytic degradation of organic dyes," *Materials Letters*, vol. 164, pp. 221–224, 2016.
- [27] C.-J. Chang, T.-L. Yang, and Y.-C. Weng, "Synthesis and characterization of Cr-doped ZnO nanorod-array photocatalysts with improved activity," *Journal of Solid State Chemistry*, vol. 214, pp. 101–107, 2014.
- [28] J. Chen, Y. Xiong, M. Duan et al., "Insight into the synergistic effect of adsorption-photocatalysis for the removal of organic dye pollutants by Cr-doped ZnO," *Langmuir: the ACS journal of surfaces and colloids*, vol. 36, no. 2, pp. 520–533, 2020.
- [29] S. N. K. Abad, M. Mozammel, J. Moghaddam, A. Mostafaei, and M. Chmielus, "Highly porous, flexible and robust cellulose acetate/Au/ZnO as a hybrid photocatalyst," *Applied Surface Science*, vol. 526, article 146237, 2020.
- [30] C. Shi, L. Zhang, H. Bian, Z. Shi, J. Ma, and Z. Wang, "Construction of Ag-ZnO/cellulose nanocomposites via tunable cellulose size for improving photocatalytic performance," *Journal of Cleaner Production*, vol. 288, article 125089, 2021.
- [31] L. M. Madikizela, "Removal of organic pollutants in water using water hyacinth (*Eichhornia crassipes*)," *Journal of Environmental Management*, vol. 295, article 113153, 2021.
- [32] D. Hemalatha, R. M. Narayanan, and S. Sanchitha, "Removal of Zinc and Chromium from industrial wastewater using water hyacinth (*E. crassipes*) petiole, leaves and root powder: Equilibrium study," *Materials Today: Proceedings*, vol. 43, pp. 1834–1838, 2021.
- [33] S. Rezanian, M. Ponraj, A. Talaiekhosani et al., "Perspectives of phytoremediation using water hyacinth for removal of heavy metals, organic and inorganic pollutants in wastewater," *Journal of Environmental Management*, vol. 163, pp. 125–133, 2015.
- [34] J. B. Neris, F. H. M. Luzardo, P. F. Santos, O. N. de Almeida, and F. G. Velasco, "Evaluation of single and tri-element adsorption of Pb²⁺, Ni²⁺ and Zn²⁺ ions in aqueous solution on modified water hyacinth (*Eichhornia crassipes*) fibers," *Journal of Environmental Chemical Engineering*, vol. 7, no. 1, article 102885, 2019.
- [35] P. Pisitsak, W. Phamonpon, P. Soontornchatchavet et al., "The use of water hyacinth fibers to develop chitosan-based biocomposites with improved Cu²⁺ removal efficiency," *Composites Communications*, vol. 16, pp. 1–4, 2019.
- [36] C. Liu, J. Ye, Y. Lin et al., "Removal of cadmium (II) using water hyacinth (*Eichhornia crassipes*) biochar alginate beads in aqueous solutions," *Environmental Pollution*, vol. 264, article 114785, 2020.
- [37] P. Kumar and M. S. Chauhan, "Adsorption of chromium (VI) from the synthetic aqueous solution using chemically modified dried water hyacinth roots," *Journal of Environmental Chemical Engineering*, vol. 7, no. 4, article 103218, 2019.
- [38] Y. Du, Q. Wu, D. Kong et al., "Accumulation and translocation of heavy metals in water hyacinth: maximising the use of green resources to remediate sites impacted by e-waste recycling activities," *Ecological Indicators*, vol. 115, article 106384, 2020.
- [39] O. A. Zelekew, S. G. Aragaw, F. K. Sabir et al., "Green synthesis of Co-doped ZnO via the accumulation of cobalt ion onto *Eichhornia crassipes* plant tissue and the photocatalytic degradation efficiency under visible light," *Materials Research Express*, vol. 8, no. 2, article 025010, 2021.
- [40] F. H. Alkallas, K. M. Elshokrofy, and S. A. Mansour, "Structural and Diffuse Reflectance Study of Cr-Doped ZnO Nanorod-Pigments Prepared via Facile Thermal Decomposition Technique," *Journal of Inorganic and Organometallic Polymers and Materials*, vol. 29, pp. 792–798, 2018.
- [41] A. Iqbal, A. Mahmood, T. Muhammad Khan, and E. Ahmed, "Structural and optical properties of Cr doped ZnO crystalline thin films deposited by reactive electron beam evaporation technique," *Progress in Natural Science: Materials International*, vol. 23, no. 1, pp. 64–69, 2013.
- [42] L. G. Mar, P. Y. Timbrell, and R. N. Lamb, "An XPS study of zinc oxide thin film growth on copper using zinc acetate as a precursor," *Thin Solid Films*, vol. 223, no. 2, pp. 341–347, 1993.
- [43] W. Han, Z. Wang, X. Li et al., "Solution combustion synthesis of nano-chromia as catalyst for the dehydrofluorination of 1,1-difluoroethane," *Journal of Materials Science*, vol. 51, no. 24, pp. 11002–11013, 2016.
- [44] A. Meng, J. Xing, Z. Li, and Q. Li, "Cr-doped ZnO nanoparticles: synthesis, characterization, adsorption property, and recyclability," *ACS Applied Materials & Interfaces*, vol. 7, no. 49, pp. 27449–27457, 2015.
- [45] X. Chen, H. Sun, J. Zhang et al., "Synthesis of visible light responsive iodine-doped mesoporous TiO₂ by using biological renewable lignin as template for degradation of toxic organic pollutants," *Applied Catalysis B: Environmental*, vol. 252, pp. 152–163, 2019.
- [46] I. Ahmad, M. Shoaib Akhtar, E. Ahmed et al., "Rare earth co-doped ZnO photocatalysts: solution combustion synthesis and environmental applications," *Separation and Purification Technology*, vol. 237, article 116328, 2020.

- [47] J. Haber, J. Stoch, and L. Ungier, "X-ray photoelectron spectra of oxygen in oxides of Co, Ni, Fe and Zn," *Journal of Electron Spectroscopy and Related Phenomena*, vol. 9, no. 5, pp. 459–467, 1976.
- [48] A. K. Worku, D. W. Ayele, N. G. Habtu et al., "Structural and thermal properties of pure and chromium doped zinc oxide nanoparticles," *SN Applied Sciences*, vol. 3, no. 7, p. 699, 2021.
- [49] N. Xuan Sang, N. Minh Quan, N. Huu Tho, N. Tri Tuan, and T. T. Tung, "Mechanism of enhanced photocatalytic activity of Cr-doped ZnO nanoparticles revealed by photoluminescence emission and electron spin resonance," *Semiconductor Science and Technology*, vol. 34, no. 2, article 025013, 2019.
- [50] M. K. Gupta, N. Sinha, and B. Kumar, "Dielectric studies and band gap tuning of ferroelectric Cr-doped ZnO nanorods," *Journal of Applied Physics*, vol. 112, no. 1, article 014303, 2012.
- [51] F. H. Alkallas, A. B. G. Trabelsi, R. Nasser, S. Fernandez, J.-M. Song, and H. Elhouichet, "Promising Cr-Doped ZnO Nanorods for Photocatalytic Degradation Facing Pollution," *Applied Sciences*, vol. 12, p. 34, 2022.
- [52] K. E. Ahmed, D.-H. Kuo, M. A. Zeleke, O. A. Zelekew, and A. K. Abay, "Synthesis of Sn-WO₃/g-C₃N₄ composites with surface activated oxygen for visible light degradation of dyes," *Journal of Photochemistry and Photobiology A: Chemistry*, vol. 369, pp. 133–141, 2019.
- [53] R. Elshypany, H. Selim, K. Zakaria et al., "Elaboration of Fe₃O₄/ZnO nanocomposite with highly performance photocatalytic activity for degradation methylene blue under visible light irradiation," *Environmental Technology & Innovation*, vol. 23, article 101710, 2021.
- [54] K. A. Isai and V. S. Shrivastava, "Photocatalytic degradation of methylene blue using ZnO and 2% Fe-ZnO semiconductor nanomaterials synthesized by sol-gel method: a comparative study," *SN Applied Sciences*, vol. 1, no. 10, p. 1247, 2019.
- [55] S. Vasantharaj, S. Sathiyavimal, P. Senthilkumar et al., "Enhanced photocatalytic degradation of water pollutants using bio-green synthesis of zinc oxide nanoparticles (ZnO NPs)," *Journal of Environmental Chemical Engineering*, vol. 9, no. 4, article 105772, 2021.
- [56] D. Paul, S. Maiti, D. P. Sethi, and S. Neogi, "Bi-functional NiO-ZnO nanocomposite: synthesis, characterization, antibacterial and photo assisted degradation study," *Advanced Powder Technology*, vol. 32, no. 1, pp. 131–143, 2021.
- [57] D. Zhu and Q. Zhou, "Environmental nanotechnology," *Monitoring & Management*, vol. 12, article 100255, 2019.
- [58] E. J. S. Christy, A. Amalraj, A. Rajeswari, and A. Pius, "Enhanced photocatalytic performance of Zr(IV) doped ZnO nanocomposite for the degradation efficiency of different azo dyes," *Environmental Chemistry and Ecotoxicology*, vol. 3, pp. 31–41, 2021.
- [59] T. K. Truong, T. Q. Nguyen, H. P. Phuong La et al., "Insight into the degradation of p-nitrophenol by visible-light-induced activation of peroxymonosulfate over Ag/ZnO heterojunction," *Chemosphere*, vol. 268, article 129291, 2021.